

GH-33637 through the Cornell Materials Science Center, Report No. 2246.

¹D. D. Osheroff, W. J. Gully, R. C. Richardson, and D. M. Lee, *Phys. Rev. Lett.* **29**, 920 (1972).

²H. Kojima, D. N. Paulson, and J. C. Wheatley, *Phys. Rev. Lett.* **32**, 141 (1974).

³A. W. Yanof, E. Smith, D. M. Lee, R. C. Richardson, and J. D. Reppy, *Bull. Amer. Phys. Soc.* **19**, 435 (1974).

⁴K. A. Shapiro and I. Rudnick, *Phys. Rev.* **137**, A1383 (1965).

⁵H. E. Hall, C. Kiewiet, and J. D. Reppy, to be published.

⁶Equation (2) may be applied to the discussion of persistent currents in a porous medium given by J. B. Mehl and W. Zimmerman, Jr., *Phys. Rev.* **167**, 214 (1968). The quantity χ defined by these authors is equal

to the coefficient $1 - \epsilon_1^2/\epsilon_2$.

⁷⁴He measurements give $n^2 = 2.53$ in our cell, 4.84 in the cell of Ref. 2. In their cell, CMN grains passed through a 35- μm sieve were packed to 80% packing fraction. In our cell 4.15 g of CMN of 50- μm average particle size was combined with 0.42 g of 1- μm Linde aluminum oxide and hand packed into the 2.96 cm^3 volume of the sample chamber. This resulted in an open volume of 0.83 cm^3 , a packing fraction of 72%.

⁸D. G. Sanikidze, I. N. Adamenko, and M. I. Kaganov, *Zh. Eksp. Teor. Fiz.* **52**, 584 (1967) [*Sov. Phys. JETP* **25**, 383 (1967)]; I. N. Adamenko and M. I. Kaganov, *Zh. Eksp. Teor. Fiz.* **53**, 615 (1967) [*Sov. Phys. JETP* **26**, 394 (1968)].

⁹T. A. Alvesalo, Yu. D. Anufriyev, H. K. Collan, O. V. Lounasmaa, and P. Wennerström, *Phys. Rev. Lett.* **30**, 962 (1973).

Time-Resolved Laser-Plasma Backscatter Studies*

B. H. Ripin, J. M. McMahon, E. A. McLean, W. M. Manheimer, and J. A. Stamper

Naval Research Laboratory, Washington, D. C. 20375

(Received 20 May 1974)

Time-resolved and time-integrated measurements of the energy, spectra, and other characteristics of the backscattered laser radiation from a laser-produced plasma are presented. Theoretical comparison shows that most of these measurements are consistent with the stimulated-Brillouin-backscattering instability.

The mechanisms responsible for absorption and reflection of laser energy in plasma are of prime importance and concern in laser fusion. The reflection of laser energy by the irradiated target represents a potentially important energy loss to the system in addition to possibly damaging the laser. A number of experimental¹⁻⁷ and theoretical⁸⁻¹¹ studies of laser backscatter indicate that an appreciable amount of energy is reflected back from the target with a modified spectrum. In this Letter we describe experiments which include both time-integrated and time-resolved energy and spectral measurements, and compare these results with stimulated-Brillouin-backscattering predictions.

The experimental setup used in these studies consists of a neodymium:glass laser beam ($\lambda_0 = 1.064 \mu\text{m}$) focused with either an $f/14$ or an $f/1.9$ lens onto a slab target in an evacuated chamber.⁴ The pulse duration used is either 900, 250, or 50 psec full width at half-maximum energy with energy ≤ 100 J. A prepulse identical in shape to the main pulse with approximately 5% of the pulse energy is usually applied 700 psec ahead of the main pulse. For the main pulse the

irradiance at the focal spot is in the range $I \leq 5 \times 10^{15} \text{ W/cm}^2$. Calorimeters independently monitor the incident energy and the energy reflected back through the lens.

A semiquantitative measurement of the angular distribution of the scattered 1.06- μm laser light at solid angles *other than back through the focusing lens* was performed.¹² By rotating the target, we determine that the intensity of this scattered radiation peaks at the specular-reflection angle from the target, has an angular extent of about $\pm 40^\circ$, and has a total energy content of 5-10% of the incident laser energy. The specularly reflected energy per solid angle is typically small compared to the direct backscattered energy. However, the total energies scattered outside and inside the solid angle subtended by the $f/14$ lens ($\pm 2^\circ$) are comparable. The fact that we independently detect specular reflection allows us to conclude that the much more intense light which is directly backscattered through the lens is the result of some anomalous process. Henceforth we will discuss only the 1.06- μm radiation backscattered through the lens solid angle.

It was verified that the backscattered light is

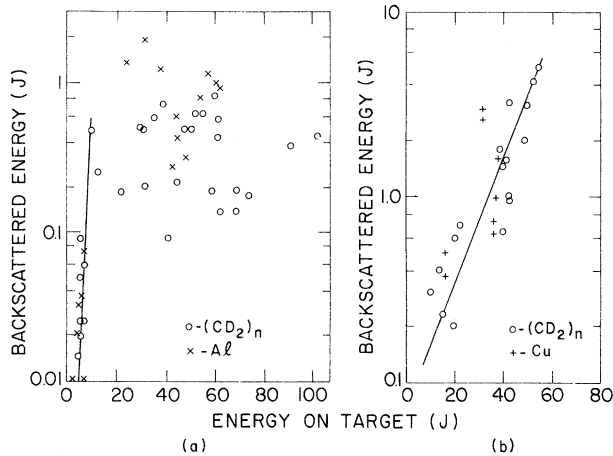


FIG. 1. Laser energy backscattered through the focusing lens near $1.06 \mu\text{m}$ versus incident energy for (a) deuterated polyethylene and aluminum slab targets, with an $f/14$ focusing lens and 900-psec (full width at half-maximum) laser pulses, and (b) deuterated polyethylene and copper slab targets, with an $f/1.9$ focusing lens and 900-psec (full width at half-maximum) laser pulses. In this plot the specular-reflection contribution (1% of the incident energy) is subtracted from the back-reflected energy.

almost completely polarized in the same plane as the incident laser beam, and that the optic rays of the backscattered radiation retraced the optic rays of the incident beam to a very high degree.³

Another property of the integrated backscattered radiation at $1.06 \mu\text{m}$ is that its total energy increases exponentially with incident laser energy up to a "saturation level" as shown in Fig. 1. A saturation occurs in the case of the $f/14$ lens, at approximately 10 J incident energy ($\sim 10^{14} \text{ W/cm}^2$) at which point $\sim 5\%$ of the energy is directly backscattered. The large scatter in the data is shot-to-shot reproducibility, not diagnostic uncertainty. The "saturation" of the energy backscattered through the lens may not imply a saturation of the total scattered radiation since considerable energy is scattered outside the sampled solid angle. An almost exponential dependence of the backscattered laser light upon incident energy is also found with the $f/1.9$ lens [Fig. 1(b)]. The behavior of the back-reflected energy has little sensitivity to the target material. However, no saturation is observed within the energy range covered with the $f/1.9$ lens. The explanation for the different behavior of the $f/1.9$ and $f/14$ lenses has not been uniquely determined as yet, although the $f/1.9$ aspheric lens produces

a smaller focal spot diameter ($\sim 30 \mu\text{m}$) than the $f/14$ plano-convex lens ($\sim 100 \mu\text{m}$) and causes a more convergent optical path.

The exponential increase of reflected energy with incident power is characteristic of the linear behavior of stimulated Brillouin backscattering if the power is such that the system is above the inhomogeneous threshold. This instability is consistent with the polarization and ray-retracing measurements. The amplification factor for power of this instability⁹ is

$$P_r \propto \exp(2\pi\gamma^2 L^2 / cv_s), \quad (1)$$

where γ is the instability growth rate near threshold given by $\gamma^2 = (\omega_{pe}^2/8)(v_{os}/v_{te})^2(v_s/c)$, L is the spatial extent for phase coherence, and c , v_s , v_{te} , and v_{os} are the speed of light, ion acoustic speed, electron thermal speed, and peak electron quiver speed in the laser field, respectively. With the assumption that the underdense plasma is isothermal, the phase coherence length L is given by

$$L^{-2} = k_i \left| \frac{2v_f}{(v_f - v_s)L_v} - \frac{\omega_{pe}^2}{(\omega^2 - \omega_{pe}^2)L_n} \right|, \quad (2)$$

where k_i is the incident laser wave number, L_n and L_v are, respectively, the plasma density and flow velocity gradient scale lengths, and v_f is the plasma flow velocity. For a typical temperature of 700 eV,⁴ and assuming interaction near one-fourth the critical density, we find that Eq. (1) gives a good fit to the exponential portion of Fig. 1(a) if we take $L = 4 \mu\text{m}$. A density gradient scale length of $30 \mu\text{m}$, a velocity gradient scale length of $200 \mu\text{m}$, and an initial fluid velocity of one-fourth the sound speed give approximately this value. The comparable number obtained for the $f/1.9$ data, adjusted for specular reflection and laser irradiance at the interaction region, is $L \approx 2.7 \mu\text{m}$.

The light reflected from the target directly back through the lens is intercepted by a pellicle beam splitter placed near the laser $\sim 34 \text{ m}$ from the target. A portion of this light is focused, with a cylindrical lens, onto the slit of a 2-m spectrograph. Time-integrated spectra from a single shot have been recorded using Kodak I-Z plates. Alternately, for time-resolved studies an EPL streak camera ($\tau_r \approx 6 \text{ psec}$) with an S-1 photocathode is used. The spectrometer is modified by masking the grating to reduce the instrumental temporal dispersion to a near time-bandwidth-limited 20 psec ($\Delta\lambda \approx 0.8 \text{ \AA}$). Spectra of the backscattered light time integrated over the laser shot showed many characteristics similar

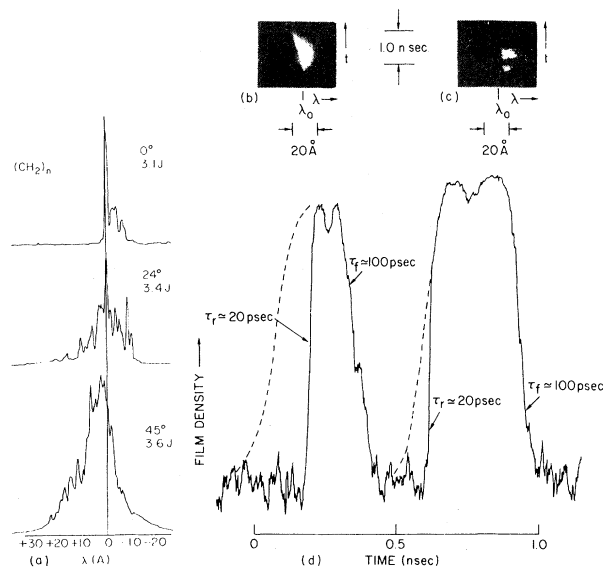


FIG. 2. (a) Shift of backscatter time-integrated spectra towards the red for an increasing angle θ between the target normal and laser direction. Time-resolved backscatter spectra for (b) a copper target, $f/14$ lens, 8.6-J, 900-psec laser pulse with 100 psec temporal resolution, and (c) a deuterated polyethylene target, $f/14$ lens, 16-J, 250-psec laser pulse with 20 psec temporal resolution. (d) Densitometer tracing of (c) along the time axis through the center of the spectrum. Traces have not been corrected for film exposure versus density curve and are saturated at the peaks.

to those obtained by other groups.^{2,3,5} Briefly, the spectra were broadened by 10–50 Å with centroids shifted from the incident wavelength (often to the blue) by up to 10 Å. It was found in our experiment, however, that as the target is rotated away from normal incidence to the laser beam the spectrum shifts toward the red. This is shown in Fig. 2(a). The magnitude of these spectral shifts with target angle are numerically consistent with a superimposed Doppler blue shift, due to plasma motion normal to the target surface ($\langle v_r \rangle \approx 4 \times 10^7$ cm/sec), and a red shift due to ion acoustic waves propagating into the target ($\Delta f \approx 7 \times 10^{11}$ Hz). The time-integrated spectra often shows a linelike structure.

The time-resolved spectra of the backscattered radiation, such as those shown in Figs. 2(b) and 2(c), show that the spectrum may evolve considerably during the laser pulse, and, therefore, correct conclusions based solely upon time-integrated spectra appear fortuitous. The slab geometry target is normal to the incident beam

in each case. A small portion of the incident-beam spectrum is monitored and it is usually found to be roughly Gaussian in time and monochromatic to within 1 Å. The backscatter spectra have varying characteristics; however, they share an initial red shift, a time-dependent spread in wavelength, a very fast rise time, and complex structure in time and wavelength. After onset the reflected energy appears distributed for the duration of the laser pulse and exhibits the laser-pulse fall time. A question arises as to why there is no cutoff threshold for instability. Both the velocity and density scale lengths increase with time in the laser-produced plasma and therefore the threshold for Brillouin backscattering would be reduced at the end of the pulse. When the incident beam is time modulated (caused by, for example, self-phase modulation) the back-reflected spectrum is similarly modulated.

There is also a tendency for the centroid of the spectra to shift increasingly to the blue with time. This is especially evident in Fig. 2(b) which exhibits a blue shift linear in time. This blue shift could occur as a result of a constant *acceleration* of the interaction region toward the laser for the duration of the shot. This is consistent with the effect of target rotation upon time-integrated spectra noted earlier. It is likely that the initial spectral red shift is due to a stimulated process such as Brillouin scattering rather than a Doppler shift since the interaction region would not have an initial net velocity away from the laser. The magnitude of the initial red shifts from the incident laser line (2–10 Å) correspond to ion acoustic wave frequencies, i.e., from 2 to 10% of the ion acoustic frequency at the critical surface. With the assumption that the usual dispersion relations for the incident and reflected electromagnetic waves ($\omega_{i,r}^2 = \omega_{pe}^2 + k_{i,r}^2 c^2$) and ion acoustic waves [$\omega_{ia} = (v_s - v_f)k_{ia}$], and the backscatter matching relations $k_r = -k_i = -\frac{1}{2}k_{ia}$, $\omega_i = \omega_r + \omega_{ia}$, hold in the interaction region, the spectral measurements lead to estimates that the interaction region is between 0.1 and 0.9 of the critical density and is typically near 0.25 of the critical density.¹³

The rapid rise time of the backscattered radiation and the existence of an intensity threshold is demonstrated in Fig. 2(d). Figure 2(d) is a densitometer tracing along the time axis through the center at the spectrum of Fig. 2(c) which shows that the rise time of the backscattering onset, due to both the laser prepulse and main pulse, is less than the resolution of the spectrometer

(~ 20 psec). When the backscattered radiation is streaked directly without going through the spectrometer the rise time still appears instrument limited (~ 6 psec). The dynamic range of the camera and film is sufficient to characterize these rise times. The broad spectrum at the onset of the backscatter spectrum in Fig. 2(c), if a result of a time-bandwidth-limited effect ($\Delta\omega\Delta\tau \simeq \frac{1}{2}\pi$ half width at half-maximum), would correspond to a rise time of about 1 psec. This 1 psec rise time is consistent with the calculated growth rate for Brillouin backscattering of $\gamma \simeq 10^{12} \text{ sec}^{-1}$ near the threshold power observed of approximately 10^{13} W/cm^2 . This threshold value is that predicted by the theory⁹ within experimental error. The threshold and intensity of backscattered radiation appears insensitive to the presence of a prepulse for all laser pulse durations used.

Another aspect of the backscattered spectra that is intriguing, but not yet satisfactorily explained, is the occasional appearance of line structure as in Fig. 2(b). These lines are rather closely spaced (~ 2 Å) and may represent multiple Brillouin backscattering. However, it is difficult to satisfy all the matching conditions except very close to the critical surface [(~ 0.96–0.98) n_c].

The bulk of our experimental evidence supports the hypothesis that stimulated Brillouin backscattering is responsible for most of the energy *directly* backscattered. Specular reflection accounts for 5–10% of the incident energy but is reduced in *intensity* with respect to the direct backscattered radiation by a large factor. An expanded study of laser light scattering will be published elsewhere.

The authors are grateful for valuable discus-

sions with J. Holzrichter, R. Shanny, K. Whitney, N. Winsor, E. Ott, H. Griem, R. Pechacek, and D. Forslund and for the expert assistance of J. Cheadle, T. DeRieux, and E. Turbyfill.

*Work supported by the U. S. Atomic Energy Commission and the Defense Nuclear Agency.

¹N. G. Basov *et al.*, *Kvantovaya Elektron.* (Moscow) 5, 63 (1972) [*Sov. J. Quantum Electron.* 2, 439 (1973)].

²J. L. Bobin, M. Decroisette, B. Meyer, and V. Yitel, *Phys. Rev. Lett.* 30, 594 (1973).

³J. F. Holzrichter *et al.*, *Bull. Amer. Phys. Soc.* 17, 972 (1972); K. Eidmann and R. Sigel, in "Laser Interaction and Related Plasma Phenomena," edited by H. Schwarz and H. Hora (Plenum, New York, to be published), Vol. 3.

⁴J. A. Stamper *et al.*, in "Laser Interaction and Related Plasma Phenomena," edited by H. Schwarz and H. Hora (Plenum, New York, to be published), Vol. 3.

⁵L. M. Goldman, J. Soures, and M. J. Lubin, *Phys. Rev. Lett.* 31, 1184 (1973).

⁶P. Lee, D. V. Giovanielli, R. P. Godwin, and G. H. McCall, *Appl. Phys. Lett.* 24, 406 (1974).

⁷J. E. Swain, *Bull. Amer. Phys. Soc.* 18, 1256 (1973).

⁸D. W. Forslund, J. M. Kindel, and E. L. Lindmann, *Phys. Rev. Lett.* 30, 739 (1973).

⁹M. N. Rosenbluth, R. B. White, and C. S. Liu, *Phys. Rev. Lett.* 31, 1190 (1973).

¹⁰H. H. Klein, W. M. Manheimer, and E. Ott, *Phys. Rev. Lett.* 31, 1187 (1973).

¹¹W. L. Kruer, K. G. Estabrook, and K. H. Sinz, *Nucl. Fusion* 13, 952 (1973).

¹²B. H. Ripin, to be published.

¹³Interpretation of red shifts from time-integrated spectra as ion acoustic waves might underestimate the ion acoustic wave frequency because of the superimposed blue Doppler shift, and place the calculated interaction region closer to the critical surface than is actually the case.

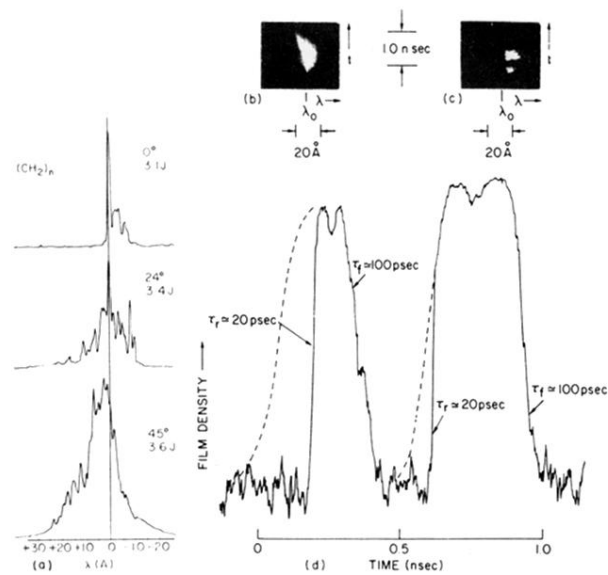


FIG. 2. (a) Shift of backscatter time-integrated spectra towards the red for an increasing angle θ between the target normal and laser direction. Time-resolved backscatter spectra for (b) a copper target, $f/14$ lens, 8.6-J, 900-psec laser pulse with 100 psec temporal resolution, and (c) a deuterated polyethylene target, $f/14$ lens, 16-J, 250-psec laser pulse with 20 psec temporal resolution. (d) Densitometer tracing of (c) along the time axis through the center of the spectrum. Traces have not been corrected for film exposure versus density curve and are saturated at the peaks.